AN ANALYSIS OF THE STORM DYNAMICS IN THE BLACK SEA

EUGEN RUSU

Abstract. The main objective of the present work is to analyze the storm dynamics in the Black Sea. A numerical wave model has been implemented and validated in the entire sea basin, including also the Sea of Azov. The wave model considered is SWAN (Simulating Waves Nearshore). This is a third generation phase averaged model based on the spectrum concept. Considering first the wind fields provided by the US National Centres for Environmental Prediction (NCEP), the above wave modelling system was used to perform an analysis of the storm conditions for the 30-year period 1987–2016. Furthermore, comparisons against satellite data show that the results of the wave predictions delivered by this system are in general accurate and reliable. As a next step, the climatic wind fields provided by the Rossby Centre regional atmospheric model were used to force this wave modelling system for the 30-year period 2021–2050. The Representative Concentration Pathway (RCP) scenario 8.5 was considered at this point. Finally, following the results concerning the wind and wave projections for the next 30 years, a comparison of the storm conditions in the past, against their expected dynamics for the near future, has been carried out. The main conclusion is that, while the intensity of the winds will increase, mainly due to the high variability expected for the wind directions the maximum values of the significant wave height will be diminished. Another observation coming from the results of this study is that the frequency of the extreme storms in the Romanian nearshore is expected to increase in the near future.

Key words: Black Sea, storms, spectral wave models, hindcast, projections, climate change.

1. INTRODUCTION

The Black Sea is an enclosed basin that can be also considered as the most distant extension of the Atlantic Ocean, via the Mediterranean Sea. The connection with the Mediterranean Sea is made via the Bosphorus Strait to the Sea of Marmara and, by extension via the Dardanelles, with the Aegean and Mediterranean seas. Although the Black Sea is an enclosed basin and the fetch is considerably smaller than in the ocean, very strong winds that usually occur in this area may generate large waves comparable with those from the ocean [1, 2].

"Dunărea de Jos" University of Galați, Romania, Department of Mechanical Engineering

Ro. J. Techn. Sci. – Appl. Mechanics, Vol. 63, N° 2, P. 127–142, Bucharest, 2018

The navigation in the Black Sea is significant, besides the already mentioned link with the Atlantic Ocean via Bosphorus, there is also a link with the North Sea by the Rhine-Main-Danube Canal. This is the main inland transportation waterway in Europe, representing the seventh Pan-European transport corridor that makes a direct connection with two major European harbours, Rotterdam in the Netherlands and Constanta in Romania [3, 4]. Since this area is subjected to high navigation conditions, it exists also an elevated risk of maritime accidents that may produce also strong impact on the environment. Furthermore, strong storms often occur in this sea and they put in real danger both navigation and many other human activities taking place either in the nearshore or offshore [5–9].

On the other hand, the climate change effects are more visible in the marine and coastal environment and moreover, these changes are very often associated with an enhancement of the intensity and the frequency of strong storms. Furthermore, many studies show that a higher dynamics in the configuration of the environmental matrix is expected in the Black Sea area in comparison with many other sea environments [10].

From this perspective, the present work has two main targets. The first is to analyze the storm dynamics in the last 30 years (the period 1987–2016). This analysis is based on validated results provided by numerical wave models. The second important objective, is to use the climatic wind models for forcing the wave modelling system in order to provide some reliable projections for the wave and wind climate in the next 30 years (the period 2021–2050). Furthermore, a comparison concerning the storm conditions that occurred in the recent past with those expected in the near future is also performed.

2. THEORETICAL ASPECTS CONCERNING SWAN MODEL

The wave model considered in the present work is SWAN, acronym from Simulating Waves Nearshore [11]. This is a third generation phase averaged wave model based on the spectrum concept, which integrates an advection type equation in fifth dimensions, which are represented by time, geographic and spectral spaces [12, 13]. The spectrum that is considered in SWAN, as in most of the spectral wave models, is the action density spectrum (N) and not the energy density spectrum. This is because in the presence of the currents, action density is conserved while energy density is not. The action density is equal to the energy density (E) divided by the relative frequency (σ).

Initially, in its early versions, this model was designed especially for the nearshore areas, as the name of the model also suggests (Simulating Waves Nearshore). During the time, the SWAN model developed a lot. This includes also the physics of the model, by including some complex processes as diffraction or wave induced set up, but also the numerical schemes associated with it [14]. These

changes also allow the application of the SWAN model to larger geographic scales. Thus, although SWAN is not so effective from the computational point of view for the oceanic areas as the large scale models, such as WAM (Wave Model) [15] or WW3 (Wave Watch 3) [16], as regards the sub oceanic scales, SWAN becomes the most appropriate model. From this perspective, as regards the wave predictions in an enclosed sea basin of average magnitude, as the Black Sea is, SWAN represents nowadays probably the most effective and reliable numerical model.

For large scale applications the governing equation (1) is expressed in the geographic space in spherical coordinates, longitude (λ) and latitude (φ), while the spectral space is defined by the relative frequency (σ) and the wave direction (θ):

$$\frac{\partial N}{\partial t}+\frac{\partial}{\partial \lambda}\dot{\lambda}N+\frac{1}{\cos\varphi}\frac{\partial}{\partial \varphi}\dot{\varphi}N\cos\varphi+\frac{\partial}{\partial \sigma}\dot{\sigma}N+\frac{\partial}{\partial \theta}\dot{\theta}N=\frac{S}{\sigma}. \tag{1}$$

S from the right-hand side of the equation (1) represents the source term. The left side of the action balance equation is the kinematic part, which reflects the propagation of the wave action in the space with fifth dimensions considering also phenomena as wave diffraction and refraction. On the right-hand side, the source term is expressed as energy density. In deep water, three components are significant. They correspond to the atmospheric input, nonlinear quadruplet interactions and whitecapping dissipation. In intermediate and shallow water some additional terms, corresponding to phenomena such as bottom friction, depth induced wave breaking and triad nonlinear wave-wave interactions may be relevant and the expression of the total source term becomes:

$$S=S_{in}+S_{nl}+S_{dis}+S_{bf}+S_{br}+S_{tr}+... \tag{2}$$

3. SWAN IMPLEMENTATION AND VALIDATION IN THE BLACK SEA

A wave modelling system, based on SWAN, has been implemented in the basin of the Black Sea and validated against both in situ and remotely sensed data [17–19]. Furthermore, the experience in implementation of the SWAN model at sub oceanic scales in some other coastal environments [20, 21], where intensive validations against in situ measurements have been performed, were also considered, both as regards the activation of the most relevant physical processes and of the model settings. From this perspective, Table 1 presents the characteristics of the computational grid and the physical processes activated in this SWAN implementation in the Black Sea basin. In this table, $\Delta\lambda$ and $\Delta\varphi$ indicate the resolution in the geographical space (for longitude and latitude, respectively), Δt is the time resolution, n_f represents the number of frequencies considered in the spectral space,

n_θ number of directions, n_λ number of grid points in longitude, n_φ number of grid points in latitude and n_p total number of grid points. The physical processes activated in the SWAN simulations, corresponding to the computational domain that covers the entire basin of the Black Sea, including also the Sea of Azov, are also presented in Table 1. In this table: Wave indicates the wave forcing, Wind the wind forcing, Td the tide forcing, Cr the current field input, Gen generation by wind, Wc the whitecapping process, Qd the quadruplet nonlinear interactions (interactions between four waves that usually occur in deep water), Tri the triad nonlinear interactions (reflecting the interactions between three waves, which are usually characteristic to intermediate and shallow water), Dif the diffraction process, B_{fr} the bottom friction, Set up the wave induced set up and Br the depth induced wave breaking. Further details concerning the performances and the accuracy of the SWAN predictions in the Black Sea, as provided by the same wave modelling system are given in [22].

Table 1
Characteristics of the computational grid and the physical processes activated in SWAN, X – process activated, 0 – process inactivated

SWAN model	*Origin*		$\Delta x \times \Delta y$ (º)		$\Delta\theta$ (º)	*Mode*		n_f	n_θ	$n_{gx} \times n_{gy} = n_p$		
Comp. grid	$X_O = 27.5°E$ $Y_O = 41.0°N$		0.08×0.08		10	*non-stat*		24	36	$176 \times 176 = 13376$		
Input / Proc.	Wave	Wind	Td	Cr	Gen	Wc	Qd	Tri	Dif	Bfr	Set up	Br
	0	X	0	0	X	X	X	0	0	X	0	X

Considering the model system configuration above presented, one of the most recent SWAN versions (SWAN 41.1) have been used in the present work. In a first approach, simulations have been carried out for the 30-year time interval 1987–2016. The wind fields provided by the US National Centres for Environmental Prediction (NCEP) have been considered for forcing the numerical wave model. The spatial resolution of the wind data is 0.325 degrees in both latitude and longitude while the temporal resolution is 3 hours. The most important wave parameters assessed are: significant wave height (H_s), wave period (T01) and mean wave direction (Dir). In order to quantify the reliability of the model predictions in terms of significant wave height, the satellite observations of the multi-mission system were considered for comparison. These comprise measurements from seven satellites: ERS-2, Poseidon, JASON-1, JASON-2, GEOSAT Follow-On (GFO), ENVISAT and TOPEX, which were used for validations.

From this perspective, Table 2 presents the statistical results obtained for the H_s values simulated with SWAN against the altimeter measurements used for validation across the Black Sea basin. The results presented are structured in two

different situations, all cases and storm waves. In this work, the storm waves are considered those for which the significant wave height is greater or equal to 3 meters. The results correspond to the 20-year time interval 1997–2016. Thus, the parameters presented in Table 2 are: bias, RMS error, scatter index (SI), correlation coefficient (R), and the regression slope (S), all of them being computed according to their standard definitions, as given below. In Table 2, n represents the number of data points considered in the statistical analysis. As it is known, the statistical quantities: bias, RMS error and scatter index are better when their values are smaller, while the correlation coefficient and the regression slope presents better results when they are closer to the unity. If X_i represent the measured values, Y_i the simulated values and n the number of observations the up mentioned parameters can be defined by the relationships:

$$X_{med} = \tilde{X} = \frac{\sum_{i=1}^{n} X_i}{n}, \quad Bias = \frac{\sum_{i=1}^{n} (X_i - Y_i)}{n}, \quad RMSE = \sqrt{\frac{\sum_{i=1}^{n} (X_i - Y_i)^2}{n}} \tag{3}$$

$$SI = \frac{RMSE}{\tilde{X}}, \quad r = \frac{\sum_{i=1}^{n} (X_i - \tilde{X})(Y_i - \tilde{Y})}{\left(\sum_{i=1}^{n} (X_i - \tilde{X})^2 \sum_{i=1}^{n} (Y_i - \tilde{Y})^2 \right)^{\frac{1}{2}}}, \quad S = \sqrt{\frac{\sum_{i=1}^{n} Y_i^2}{\sum_{i=1}^{n} X_i^2}} \tag{4}$$

At this point, it has to be also highlighted that for the total data results presented in Table 2, the average simulated value for the significant wave height is 1.0 m while the average measured value is 1.05 m. On the other hand, for the storm waves the average simulated H_s value is 3.75 m while the average measured value is 3.68 m. It can be also noticed that the storm waves represent about 2% of the total.

Finally, it can be concluded that the statistical results presented in Table 2 show that in general the SWAN predictions are reasonable both as regards the average and the storm conditions. The results corresponding to the statistical data presented in Table 2 are also illustrated in Fig. 1. This provides the scatter diagram for the significant wave height (simulations against measurements) for the two different situations considered, total data and storm waves. The two plots presented in Fig. 1 also indicate that the SWAN results are in general reliable for both average energy and storm conditions. This gives also a good degree of credibility to the analyses related to the past and future storm conditions in the Black Sea, which will be presented next.

Table 2

H_s statistics, SWAN against the satellite data corresponding to the time interval 1997–2016

Parameter (m)	Bias (m)	RMS (m)	SI	r	S	N
H_s – total data	0.05	0.38	0.36	0.87	0.99	1174657
H_s >3 m	-0.07	0.67	0.21	0.78	1.05	23841

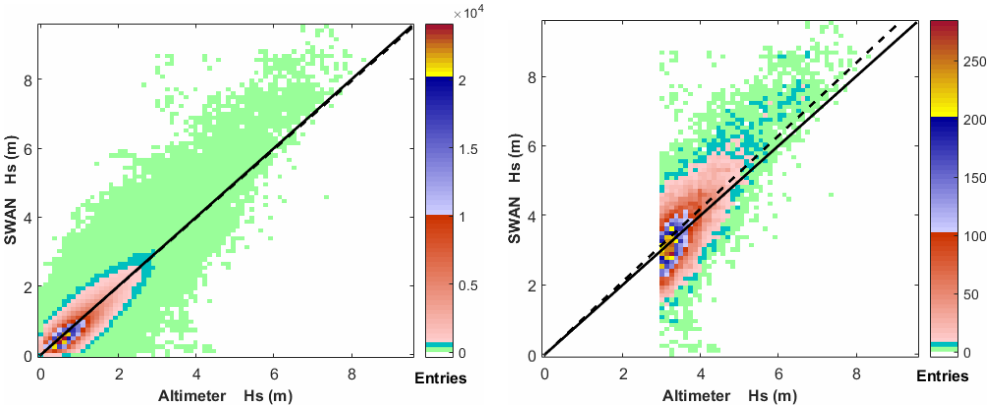

a) b)

Fig. 1 – H_s scatter diagrams: a) total data; b) storm conditions (H_s > 3 m).

4. ANALYSIS OF THE STORM DYNAMICS IN THE RECENT PAST (1987–2016)

In order to provide a comprehensive picture of the storm conditions corresponding to the recent past in the Black Sea basin, the results of the SWAN modelling system for the 30-year period 1987–2016 will be analyzed next. Thus, Fig. 2 illustrates the H_s annual maximum series for this 30-year time interval 1987–2016. The maximum values of the wind speed are also indicated.

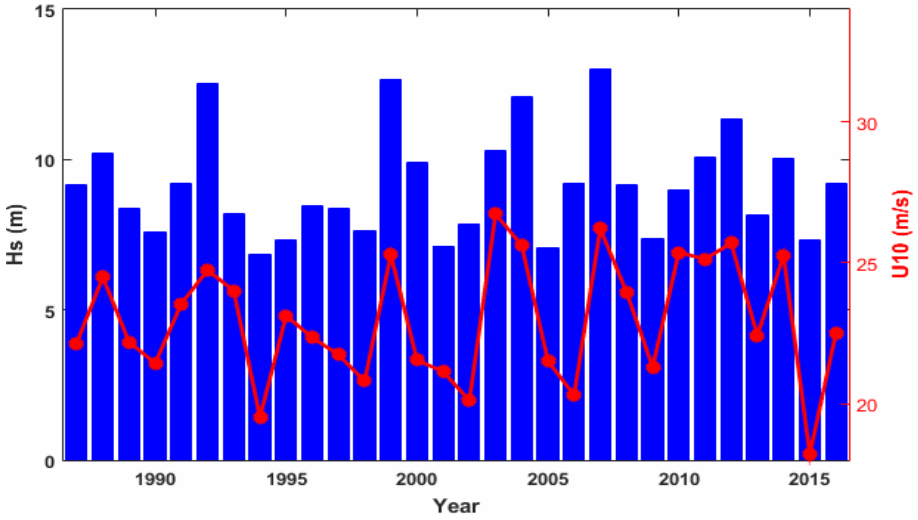

Fig. 2 – H_s annual maximum series corresponding to the 30-year time interval 1987–2016, the maximum values of the wind speed are also indicated.

From Fig. 2, it can be noticed that the maximum H_s value was registered in 2007/11/11. This maximum significant wave height was greater than 13 meters (13.03 m). According to the Rayleigh distribution, it means that maximum wave heights even of 25 meters have been formed at that time. The corresponding maximum wind speed for the respective time frame in the Black Sea basin was 26.2 m/s. Further on, Fig. 3 illustrates the H_s monthly maximums for the same 30-year time interval. The exact values of the significant wave height and of the wind speed at 10 meters height above the sea level U10 as well as the locations of the maximum monthly significant wave height are also given in Table 3.

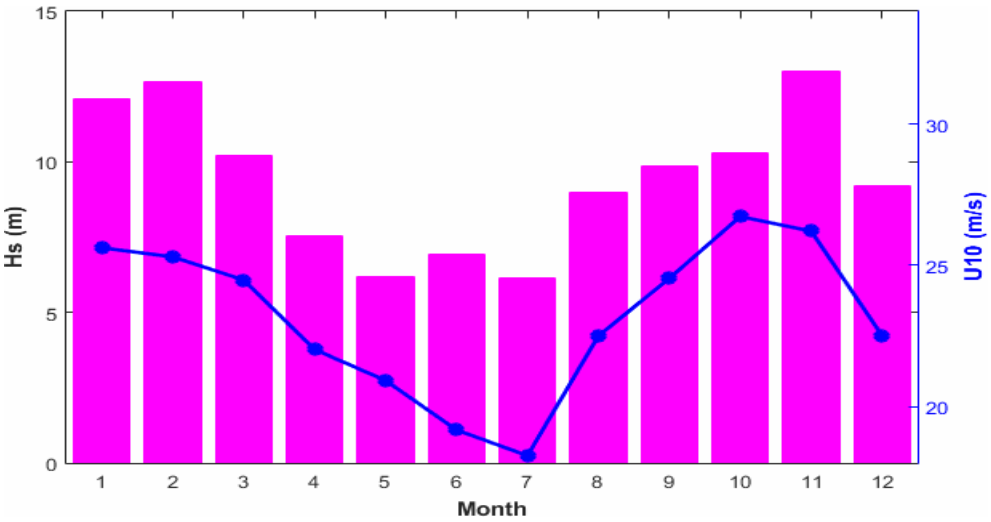

Fig. 3 – H_s monthly maximums corresponding to the 30-year time interval 1987–2016, the maximum values of the wind speed are also represented.

Table 3
Values and locations of the maximum monthly significant wave height corresponding to the 30-year time interval 1987–2016

Month	*Date*	*Long* (°)	*Lat* (°)	H_s (m)	U10 (m/s)
January	2004/01/22	29.82	41.72	12.10	25.62
February	1999/02/06	39.18	42.60	12.67	25.30
March	1998/03/03	33.10	44.76	10.20	24.48
April	2012/04/14	31.58	44.36	7.55	22.02
May	2008/05/29	37.26	42.12	6.18	20.92
June	2001/06/05	35.42	42.92	6.91	19.17
July	2013/07/02	35.74	42.44	6.15	18.26
August	2011/08/12	29.50	41.64	8.98	22.50
September	2014/09/24	35.82	42.44	9.84	24.54
October	2003/10/09	34.38	43.16	10.29	26.73
November	2007/11/11	34.46	44.12	13.03	26.21
December	2016/12/19	30.30	41.64	9.20	22.51

5. PROJECTIONS FOR THE EXPECTED STORM DYNAMICS IN THE NEAR FUTURE (2021–2050)

The next step was to perform projections concerning the expected storm conditions in the basin of the Black Sea corresponding to the near future time interval (2021–2050). For this reason, the same wave modelling system was considered, but this time climatic wind fields were used to force the model. The wind fields used at this step are those coming from the Rossby Centre regional atmospheric model provided by the Swedish Meteorological and Hydrological Institute The version RCA4 predicted under the Representative Concentration Pathway (RCP) scenario 8.5 used in Climate Model Intercomparison Project phase 5 (CMIP5) [23] is next considered. As regards the RCP scenarios, these are described in [24], where an overview of the most relevant model configurations, forcing, and initialization procedures is provided. Thus, it was found that the climate feedback significantly depends on the global warming and also probably on the history of the forcing. The global warming considers as a climatologically base the year 1850 and goes up to 2080–2100. The four RCP scenarios are RCP2.6, RCP4.5, RCP6, and RCP8.5. They are named after the possible range of radiative forcing values in the year 2100 relative to the pre-industrial values. Thus, RCP 2.6 assumes that the global annual greenhouse gas emissions (measured in CO_2-equivalents) will have a peak in the interval 2010–2020, with emissions declining substantially thereafter. In such case, at the end of the century a temperature increase of about 1.5 °C is expected, while the radiative forcing value will be about 2.6 W/m^2. In RCP 8.5, it is assumed that emissions continue to rise throughout the 21st century and an increase of about 4.4°C is expected until 2100 with a radiative forcing value that will exceed 8.5 W/m^2. The spatial resolution of this wind field is 0.11 degrees, while the time step is 6 hours.

Thus, Fig. 4 illustrates the H_s annual maximum series expected for the 30-year time interval 2021–2050. The maximum values of the wind speed are also indicated. From Fig. 4, it can be noticed that the maximum H_s value it is expected in 2040/10/28. This maximum significant wave height it would be around 11.5 meters. The corresponding maximum wind speed for the respective time frame in the Black Sea basin it is expected to be about 30.75 m/s. Furher on, Fig. 5 illustrates the H_s monthly maximums expected in the same 30-year time interval. The exact values of the significant wave height and of the wind speed at 10 meters height above the sea level (U10) as well as the locations of the maximum monthly significant wave height are also given in Table 4.

Table 4
Values and locations of the maximum monthly significant wave height expected in 30-year time interval 2021–2050

Month	*Date*	*Long* (°)	*Lat* (°)	H_s (m)	U10 (m/s)
January	2022/01/24	36.22	44.60	7.62	21.05
February	2042/02/06	37.90	44.36	9.74	27.26
March	2031/03/31	33.10	44.04	9.84	22.28

Table 4 (continued)

April	2031/4/01	34.38	43.88	9.12	21.54
May	2050/05/13	30.46	43.16	6.40	19.58
June	2038/06/25	38.30	44.04	5.80	22.79
July	2038/07/03	37.10	44.20	6.04	22.71
August	2033/08/23	32.62	43.08	4.38	18.00
September	2025/09/27	29.50	44.12	10.93	32.70
October	2040/10/28	38.38	44.04	11.45	30.75
November	2047/11/11	37.74	44.44	10.89	30.60
December	2026/12/11	29.34	43.64	8.36	23.33

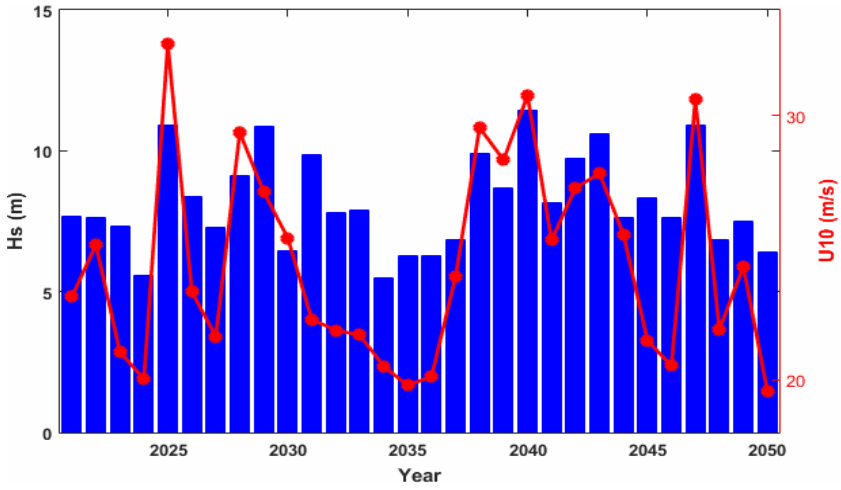

Fig. 4 – H_s annual maximum series expected in the 30-year time interval 2021–2050, the maximum values of the wind speed are also represented.

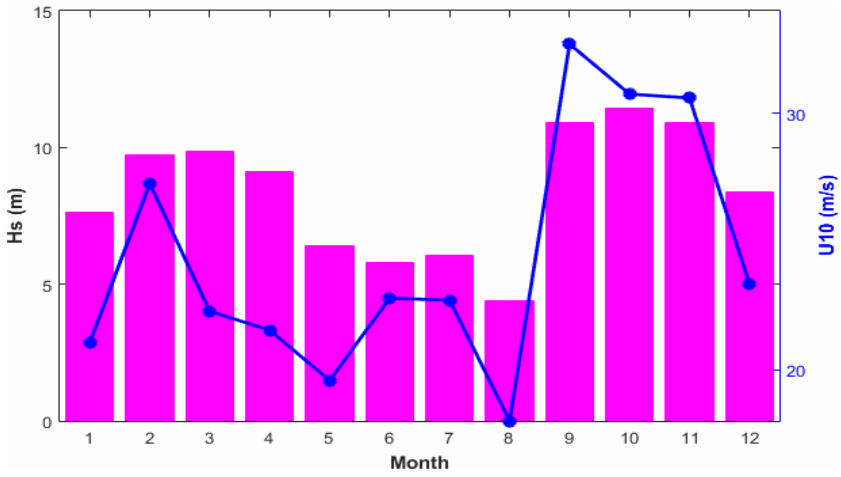

Fig. 5– H_s monthly maximums expected in the 30-year time interval 2021–2050, the maximum values of the wind speed are also represented.

6. DISCUSSION

At this point, a discussion will be employed in relationship with the storm conditions encountered in the recent past against those expected in the near future. Thus, the results presented in Figure 2 show that in the 30-year time interval 1987–2016 in nine years significant wave heights greater than 10 meters have been noticed. These are: 1988 (H_s = 10.2 m), 1992 (H_s = 12.54 m), 1999 (H_s = 12.67 m), 2003 (H_s = 10.29 m), 2004 (H_s = 12.1 m), 2007 (H_s = 13.03 m), 2011 (H_s = 10.1 m), 2012 (H_s = 11.37 m) and 2014 (H_s = 10.04 m). On the other hand, in the next 30-year period only in five years we expect significant wave heights greater than 10 meters. These are: 2025 (H_s = 10.93 m), 2029 (H_s = 10.88 m), 2040 (H_s = 11.45 m), 2043 (H_s = 10.62 m) and 2047 (H_s = 10.89 m). Comparing these values we can conclude not only that from the point of view of the significant wave height the number of the extreme storms will decrease, but also the maximum values of the significant wave height is expected to be decreased in the near future period. If we look at the maximum values of the wind speed corresponding to the time frames when we have maximum significant wave heights, we can notice wind speeds greater than 25 m/s only in eight years: 1999 (U10 = 25.29 m/s), 2003 (U10 = 26.73 m/s), 2004 (U10 = 25.62 m/s), 2007 (U10 = 26.21 m/s), 2010 (U10 = 25.37 m/s), 2011 (U10 = 25.13 m/s), 2012 (U10 = 25.70 m/s) and 2014 (U10 = 25.27 m/s). At the same time, for the near future period (2021–2050) we expect wind field velocities greater than 25 m/s more often (13 times), that is in the years: 2022 (U10 = 25.11 m/s), 2025 (U10 = 32.70 m/s), 2028 (U10 = 29.36 m/s), 2029 (U10 = 27.1 m/s), 2030 (U10 = 25.37 m/s), 2038 (U10 = 29.54 m/s), 2039 (U10 = 28.32 m/s), 2040 (U10 = 30.75 m/s), 2041 (U10 = 25.28 m/s), 2042 (U10 = 27.26 m/s), 2043 (U10 = 27.81 m/s), 2044 (U10 = 25.50 m/s) and 2047 (U10 = 30.6 m/s). At this point it can be also noticed that while the maximum wind speed value that corresponds to the annual maximum H_s series is 26.73 m/s in the past (for the time frame 2003/10/09), in the future this value is exceeded several times, as follows: 2025/09/27, 2028/02/11, 2029/11/15, 2038/11/05, 2039/10/28, 2040/10/28, 2042/02/06, 2043/11/10, 2047/11/11 with the corresponding wind speeds (32.7 m/s, 29.36 m/s, 27.1 m/s, 29.54 m/s, 28.32 m/s, 30.75 m/s, 30.75 m/s, 27.26 m/s, 27.81 m/s, 30.6 m/s). Furthermore, if we compute the average values for significant wave height and wind speed maximums, it will result mean H_s = 9.2m and mean U10 = 22.9 m/s for the 30-year time interval 1987–2016, while for the interval 2021–2050 the expected corresponding values are mean H_s = 8.2 m and mean U10 = 24.4 m/s.

At a first look, this result seems contradictory because a clear increase of the wind speed intensity is followed by a clear decrease of the significant wave height in the near future period 2021–2050. Interesting conclusions result also from the

analysis of Fig. 6. This figure illustrates the geographical location of H_s annual maximums registered in the 30-year time interval 1987–2016, represented by yellow circles against the H_s annual maximums expected in the 30-year time interval 2021–2050, represented by magenta circles. From the analysis of the locations of the annual maximums as registered in the recent past against those expected in the near future, we can notice a tendency of migration of the storms from the south and the centre of the sea to the west and to the north.

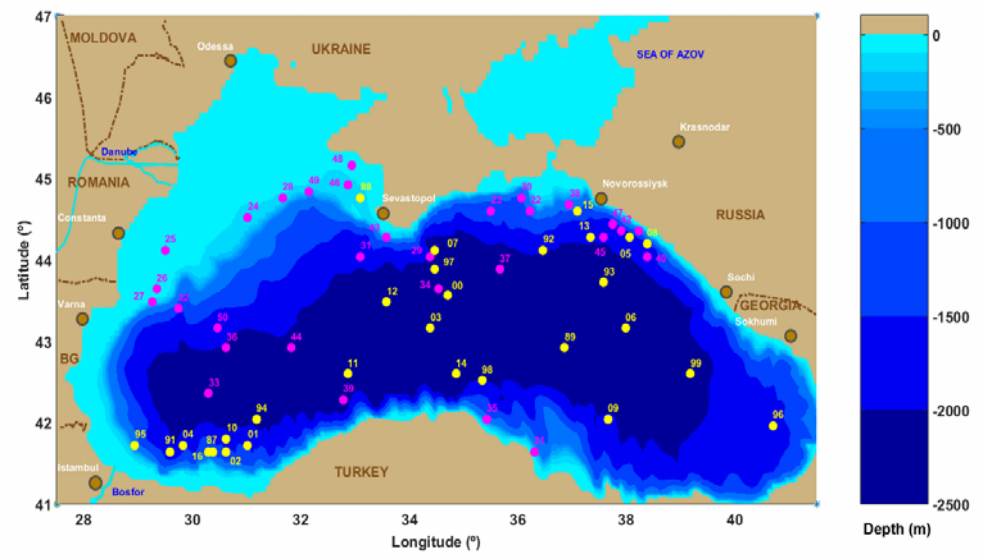

Fig. 6 – Geographical location of H_s annual maximums registered in the 30-year time interval 1987–2016, represented by yellow circles against the H_s annual maximums expected in the 30-year time interval 2021–2050, represented by magenta circles.

Finally, by analyzing the results presented in Tables 3 and 4, we can also notice that the highest storms were registered in the recent past in the months: November, January and February, while in the near future we expect the highest storms in September, October and November.

The highest three annual storms will be analyzed next, presenting also the spatial distributions of the significant wave height and of the corresponding wind fields in the geographical space. The time frames resulted in the 30-year interval 1987–2016 are 2007/11/11 (H_s = 13.03 m, U10 = 26.21 m/s), 1999/02/20 (H_s = 12.67 m, U10 = 25.29 m/s) and 1992/11/15 (H_s = 12.54 m, U10 = 24.74 m/s). The significant wave height scalar fields and the wave vectors for these top three storms of the 30-year time interval 1987–2016 are illustrated in Figs. 7a, 7c and 7e, respectively. The locations of the storm peaks are illustrated in these subplots with white circles.

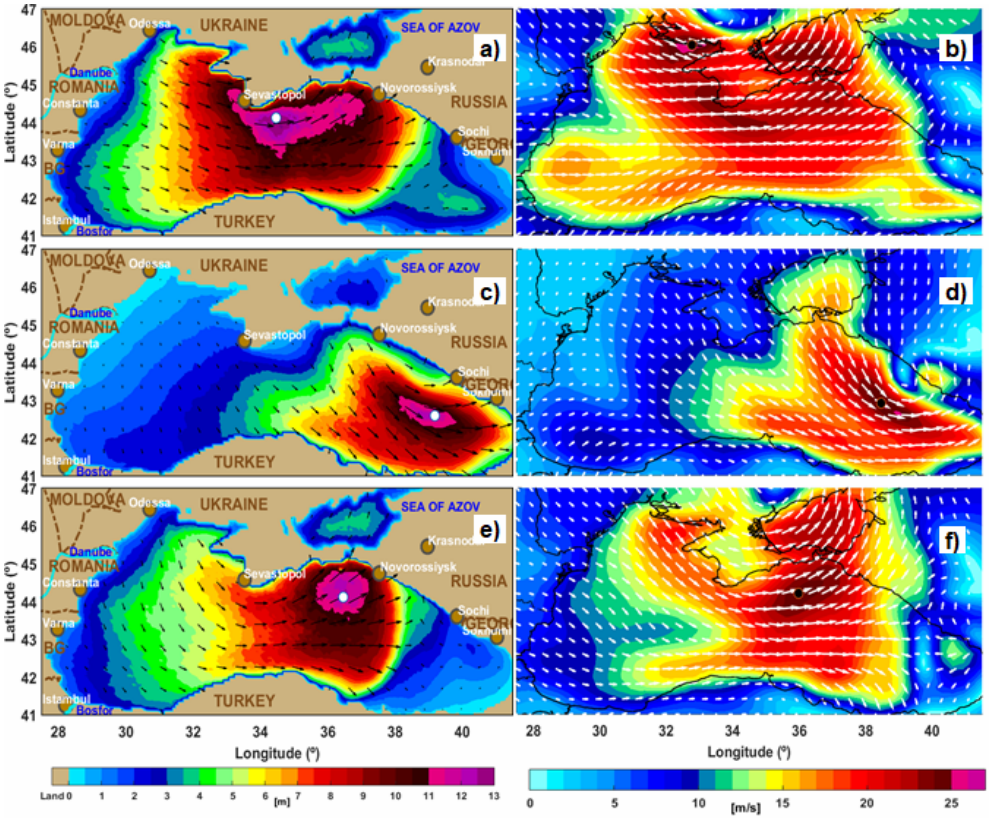

Fig. 7 – Significant wave height fields (H_s) and wave vectors for the top three storms of the 30-year time interval 1987–2016. The time frames are: a) 2007/11/11-h09; c) 1999/02/20-h06; e) 1992/11/15-h09. The corresponding scalar wind fields and wind velocity vectors (U10) for the top three storms: b) 2007/11/11-h09; d) 1999/02/20-h06; f)1992/11/15-h09.

It can be noticed that the peaks of the storms illustrated in Figs. 7a and 7e are located in the northern side of the Black Sea, while in the case presented in Fig. 7c the peak is located in north-eastern side of the sea. Figures 7b, 7d and 7f present the corresponding scalar wind fields and wind velocity vectors (U10) for these top three storms. An important aspect to be noticed is that, although the dominant pattern for the wind blowing in the basin of the Black Sea is from the northeast, all these three major storms correspond to the wind blowing from the northeast.

As regards the expected annual storms in the near future period, the time frames considered are 2040/10/28 (H_s = 11.45 m, U10 = 30.75 m/s), 2025/09/27 (H_s = 10.93 m, U10 = 32.70 m/s) and 2047/11/11 (H_s = 10.89 m, U10 = 30.6 m/s). The significant wave height scalar fields and the wave vectors for these expected top three storms of the 30-year time interval 2021–2050 are illustrated in Figs. 8a, 8c and 8e.

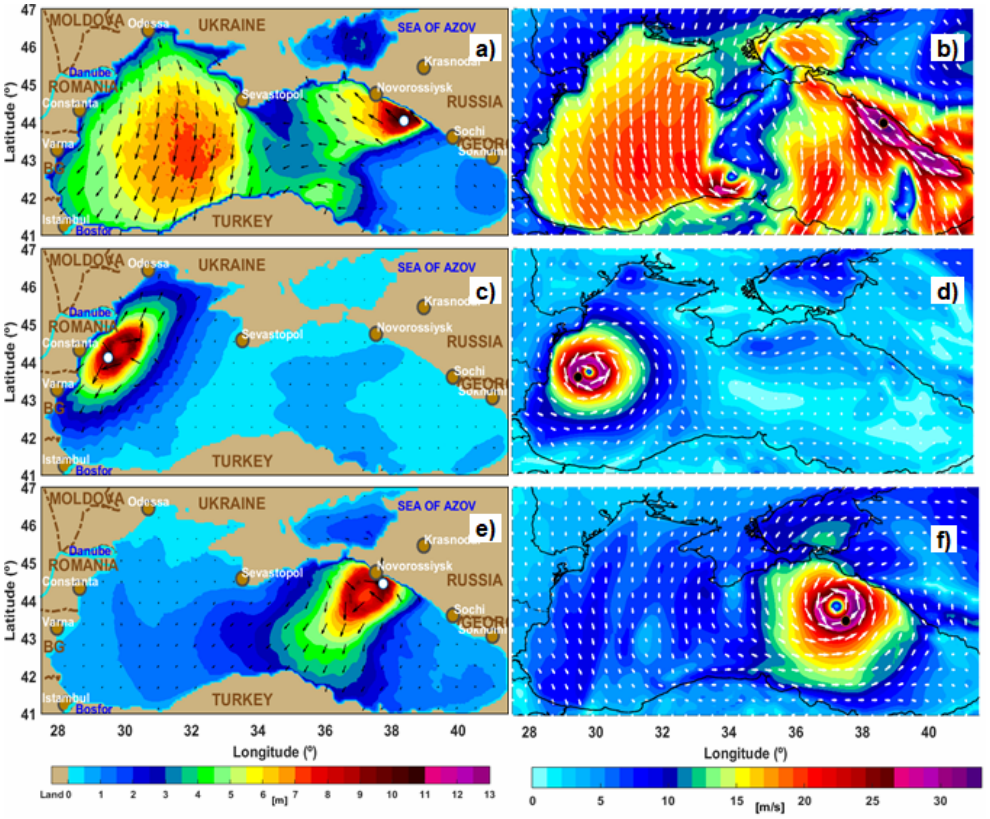

Fig. 8 – Significant wave height fields (H_s) and wave vectors for the expected top three storms of the 30-year time interval 2021–2050. The time frames considered are: a) 2040/10/28-h06; c) 2025/09/27-h18; e) 2047/11/11-h12. The corresponding scalar wind fields and wind velocity vectors (U10) for the top three storms: b) 2040/10/28-h06; d) 2025/09/27-h18; f) 2047/11/11-h12.

The locations of the storm peaks are also indicated in these subplots with white circles. Looking at these figures, we can notice that for the storms presented in Figs. 8a and 8e, the peaks are located in the northern side of the sea, very close to the coast. Moreover, both peaks are located not far from each other, close to the Russian city Novorossiysk. On the other hand, the storm peak illustrated in Fig. 8c appears to be on the western side of the sea very close to the Romanian nearshore. Very interesting results come from the analysis of the wind fields presented in Figs. 8b, 8d and 8f. In all these cases, the maximum value of the wind speed is higher than 30 m/s. Moreover, in all three cases we can see a cyclonic behaviour in the spatial distribution of the wind field. However, while in the case illustrated in Fig. 8b the storm covers the entire sea basin and the cyclone is located in the southern side of the sea, far away from the peak of the storm, in the other two cases (illustrated in Figs. 8d and 8f), the storm peak is located practically inside the

cyclone. Moreover, in these last two cases the storms, although very strong, are quite local and the rest of the sea appears to be almost calm. The effect of this high variability in the wind directions, which can be noticed in all the three cases presented in Fig. 8, is that although the wind speeds are very high (much higher than in the cases presented in Fig. 7), the resulting maximum values of the significant wave height are lower than in the extreme cases corresponding to the recent past. This is because the wind field configurations expected for the extreme storms from the near future indicate a high variability of the wind direction, which reduces the fetch and does not allow the development of the very high waves as those characteristic to the recent past.

7. CONCLUSIONS

The objective of this work was to analyze the storm conditions in the Black Sea. As a first step, using a validated modelling system a 30-year hindcast, covering the time interval 1987–2016, has been performed. In this way, the main storms that occurred in the recent past have been identified and analyzed. The next step was to perform projections concerning the expected storm conditions in the basin of the Black Sea corresponding to the near future time interval (2021–2050). For this reason, the same wave modelling system was considered, but this time the climatic wind fields were used to force the model.

From the analysis of the results, we can notice first that the extreme storm waves are higher in the recent past that there will be expected in the near future. Thus, the analysis of the annual maximum series shows that in the period 1987–2016, there were four years with maximum significant wave heights greater than 12 meters (1992, 1999, 2004 and 2007) while in the near future, covering the 30-year period 2021–2050, no such situation is expected, the maximum value of the significant wave height predicted for the entire 30-year period being 11.45 m. On the other hand, a substantial increase in terms of the maximum wind speed is expected in the near future, when comparing with the recent past. Thus, an increase in terms of the maximum wind speed of about 5 m/s is expected while in three years the maximum wind speed would be even greater than 30 m/s. On the other hand, it has to be highlighted that the cyclonic forms that are often noticed in the climatic wind fields for the extreme storms expected in the near future do not favour the enhancement of the waves, because of the sudden changes of the wind directions. Such wind behaviour limits the fetch over which the extreme waves are generated and that is why the substantial enhancements in terms of the wind speed are not followed by an increase in terms of significant wave height. On the contrary, because of these limited fetches, according to the results presented, the extreme waves expected in the near future will be smaller in terms of significant wave heights than in the past.

From the analysis of the results, another tendency that is noticed for the near future period is a migration of the location of the peak storms from the southwest and the centre of the sea to the west and the north, coming closer to the coastal environment in the northern part of the Black Sea. Finally, it has to be also highlighted that the future climate projections have been made in the present work under the hypothesis of the RCP8.5 scenario, while if considering the RCP2.6 scenario, moderate changes in terms of the wind speed are expected.

Acknowledgements. The author gratefully acknowledges that this work was carried out in the framework of the project ACCWA (Assessment of the Climate Change effects on the WAve conditions in the Black Sea), supported by the Romanian Executive Agency for Higher Education, Research, Development and Innovation Funding – UEFISCDI, grant number PN-III-P4-ID-PCE-2016-0028.

Received on July 9, 2018

REFERENCES

1. VALCHEV, Nikolay, DAVIDAN, Izrail, BELBEROV, Zdravko, PALAZOV, Atanas, VALCHEVA, Nadezdha, *Hindcasting and assessment of the western Black Sea wind and wave climate*, J. Env. Prot. Ecology, **11**, pp. 2001–2012, 2010.
2. RUSU, Liliana, BUTUNOIU, Dorin, RUSU, Eugen, *Analysis of the extreme storm events in the Black Sea considering the results of a ten-year wave hindcast*, Journal of Environmental Protection and Ecology, **15**, *2*, pp. 445–454, 2014.
3. IVAN, Angela, GASPAROTTI, Carmen, RUSU, Eugen, *Influence of the interactions between waves and currents on the navigation at the entrance of the Danube Delta*, J. Environ. Prot. Ecol., **13**, pp. 1673–1682, 2012.
4. GASPAROTTI, Carmen, RUSU, Eugen, *Methods for the risk assessment in maritime transportation in the Black Sea basin*, Journal of Environmental Protection and Ecology – Special Issue: Protection and Sustainable Management of the Black Sea Ecosystem, **13**, *3A*, pp. 1751–1759, 2012.
5. MAKRIS, C., GALIATSATOU, P., TOLIKA, K., ANAGNOSTOPOULOU, C., KOMBIADOU, K., PRINOS, P., VELIKOU, K., KAPELONIS, Z., TRAGOU, E., ANDROULIDAKIS, Y., ATHANASSOULIS, G., *Climate change effects on the marine characteristics of the Aegean and Ionian Seas*, Ocean Dynamics, **66**, *12*, pp. 1603–1635, 2016.
6. VLASCEANU, Elena, NICULESCU, Dragos, OMER, Ichinur, et al., *Offshore wave regime investtigations towards safety port operations in the transitional zone of the Romanian coast*, SGEM 2015 GeoConference on Water Resources, Forest, Marine and Ocean Ecosystems, Vol. II, pp. 675–682, 2015.
7. RUSU, Eugen, GUEDES SOARES, Carlos, *Modelling the effect of wave current interaction at the mouth of the Danube river*, Developments in Maritime Transportation and Exploitation of Sea Resources, Vol. 2, pp. 979–986, 2014.
8. VLASCEANU, Elena, OMER, Ichinur, NICULESCU, Dragos, et al. *Modeling aspects of the hydro-geomorphological process and their impact on the evolution of the Romanian coastal eco-system on the Black Sea, in the context of the new climate change*, SGEM 2015 Geo Conference on Water Resources, Forest, Marine and Ocean Ecosystems, Vol. II, pp. 667–674, 2015.
9. OMER, Ichinur, MATEESCU, Razvan, VLASCEANU, Elena, et al., *Hydrodynamic regime analysis in the shore area taking into account the new master plan implementation for the coastal*

protection at the Romanian shore, SGEM 2015 GeoConference on Water Resources, Forest, Marine and Ocean Ecosystems, vol. II, pp. 651–657, 2015.
10. ONEA, Florin, RUSU, Liliana, *A long-term assessment of the Black Sea wave climate*, Sustainability, **9**, *10*, p. 1875, 2017.
11. BOOIJ, N., RIS, R., HOLTHUIJSEN, L., *A third generation wave model for coastal regions. Part 1: Model description and validation*, J. Geophys. Res., **104**, *C4*, pp. 7649–7666, 1999.
12. HOLTHUIJSEN, Leo, *Waves in oceanic and coastal waters*, Cambridge University Press, 2007.
13. RUSU, Eugen, *Strategies in using numerical wave models in ocean/coastal applications*, Journal of Marine Science and Technology, **19**, *1*, pp. 58–75, 2011.
14. SWAN team, *Scientific and technical documentation*, SWAN Cycle III, Delft University of Technology, Department of Civil Engineering, the Netherlands, 2017.
15. WAMDI Group, *The WAM model – A third generation ocean wave prediction model*, J. Phys. Oceanogr., **18**, *12*, pp. 1775–1810, 1988.
16. TOLMAN, Hendrik, *A third-generation model for wind waves on slowly varying, unsteady and inhomogeneous depths and currents*, J. Phys. Oceanogr., **21**, *6*, pp. 782–797, 1991.
17. RUSU, Eugen, *Wave energy assessments in the Black Sea*, Journal of marine science and technology, **14**, *3*, pp. 359–372, 2009.
18. RUSU, Liliana, BERNARDINO, Mariana, GUEDES SOARES, Carlos, *Wind and wave modelling in the Black Sea*, Journal of Operational Oceanography, **7**, *1*, pp. 5–20, 2014.
19. RUSU, Liliana, IVAN, Angela, *Modelling wind waves in the Romanian coastal environment,* Environmental Engineering and Management Journal, **9**, *4*, pp. 547–552, 2010.
20. RUSU, E., VENTURA SOARES, C., RUSU, L., *Computational strategies and visualization techniques for the waves modeling in the Portuguese nearshore*, Maritime Transportation and Exploitation of Ocean and Coastal Resources, **2**, pp. 1129–1136, 2005.
21. RUSU, E., SOARES, C.V., PINTO, J.P. SILVA, R., *Extreme events and wave forecast in the Iberian nearshore*, Coastal Engineering (4 volumes), pp. 727–739, 2004.
22. RUSU, Eugen, *Reliability and Applications of the Numerical Wave Predictions in the Black Sea*, Frontiers in Marine Science, **3**, pp. 1–13, 2016.
23. GIORGETTA, Marco, JUNGCLAUS, Johann, REICK, Christian, LEGUTKE, Stephanie, et al., *Climate and carbon cycle changes from 1850 to 2100 in MPI–ESM simulations for the Coupled Model Intercomparison Project phase 5*, Journal of Advances in Modeling Earth Systems, **5**, *3*, pp. 572–597, 2013.
24. MOSS, Richard H., EDMONDS, Jae A., HIBBARD, Kathy A., MANNING, Martin R., ROSE, Steven K., et al., *The next generation of scenarios for climate change research and assessment*, Nature, **463**, *7282*, pp. 747–756, 2010.